Microchimica Acta (2020) 187: 400
https://doi.org/10.1007/s00604-020-04323-6

ORIGINAL PAPER

Dual metal cations coated magnetic mesoporous silica probe for highly selective capture of endogenous phosphopeptides in biological samples

Xufang Hu[1] · Yilin Li[1] · Aizhu Miao[2] · Chunhui Deng[1]

Received: 12 December 2019 / Accepted: 14 May 2020 / Published online: 22 June 2020

Abstract

For the first time, dual metal ions (Ti^{4+}-Zr^{4+}) were successfully modified into the channel of magnetic mesoporous silica to obtain an affinity probe for highly selective capture of endogenous phosphopeptides in biological samples. The newly prepared Fe_3O_4@$mSiO_2$@Ti^{4+}-Zr^{4+} composites possessed the advantages of ordered mesoporous channels, superparamagnetism, and enhanced affinity properties of dual metal ions of Ti^{4+} and Zr^{4+}. The phosphopeptide enrichment efficiency of the Fe_3O_4@$mSiO_2$@Ti^{4+}-Zr^{4+} composite was investigated, and the result indicated an ultrahigh size exclusive ability (weight ratio of β-casein tryptic digests, BSA, and α-casein protein reached up to 1:1000:1000). Compared to magnetic affinity probes with single metal ions (Fe_3O_4@$mSiO_2$@Ti^{4+}, Fe_3O_4@$mSiO_2$@Zr^{4+}), the composite possessed stronger specificity, higher sensitivity, and better efficiency; and more importantly, it showed much enhanced enrichment ability towards both mono- and multi-phosphorylated peptides. Additionally, by utilizing the Fe_3O_4@$mSiO_2$@Ti^{4+}-Zr^{4+} affinity probe, a total number of 104 endogenous phosphopeptides including 95 mono-phosphopeptides and 9 multi-phosphopeptides were captured and identified from human saliva, indicating the great potential for the application of the novel probe for the peptidome analysis in the future.

Keywords Endogenous phosphopeptide · Molecular recognition · Magnetic mesoporous probe · Dual metal cations affinity

Introduction

Peptidome, which is defined as the low-molecular-weight part of the proteome, has been considered a source of biomarkers for the diagnostics, for they consist many bioactive peptides including peptide hormones, endogenous peptide products, and potentially bioactive degradation from the parent proteome [1]. Endogenous peptides can derive from a regulated process which would represent the proteins with post-translational maturation [2]. Thus, the endogenous peptides with post-translational modifications (PTMs) can also provide important information [3]. As one of the most important post-translational modifications, phosphorylation plays a significant role in many biological processes, such as cell growth, differentiation, and apoptosis [4]. Thus, the studies of phosphopeptidomics in human biofluids hold great research value for the disease biomarker discovery. However, the traditional mass spectrometry (MS) method in the profiling of endogenous phosphopeptides still faces big challenges, because of the low content and poor ionization efficiency of endogenous phosphopeptides in samples and the serious signal suppression from high abundance proteins [5, 6]. Therefore, it is imperative to explore effective strategy to enrich endogenous phosphopeptides before the MS analysis [7–9].

Electronic supplementary material The online version of this article (https://doi.org/10.1007/s00604-020-04323-6) contains supplementary material, which is available to authorized users.

✉ Aizhu Miao
aizhu.miao@fdeet.org

✉ Chunhui Deng
chdeng@fudan.edu.cn

[1] Department of Chemistry, Department of Gastroenterology and Hepatology, Zhongshan Hospital, Institutes of Biomedical Sciences, Collaborative Innovation Center of Genetics and Development, Fudan University, Shanghai 200433, China

[2] Department of Ophthalmology and Vision Science, Eye and ENT Hospital, NHC Key Laboratory of Myopia, Fudan University, Shanghai, China

Nowadays, numerous strategies were employed to enrich phosphopeptides from complex biosamples, such as SPE [10], ion exchange chromatography (IEC) [11], metal oxide affinity chromatography (MOAC) [12–14], and immobilized metal ion affinity chromatography (IMAC) [15, 16]. Since 1986, Fe^{3+}-immobilized iminodiacetate-agarose gel was employed to isolate phosphoproteins in Andersson's group [17]. Immobilized metal affinity chromatography (IMAC) has been widely used for the phosphoproteomics profiling for a long time. To date, a large number of metal cations including Cu^{2+}, Zn^{2+}, Fe^{3+}, Ga^{3+}, Al^{3+}, Ti^{4+}, and Zr^{4+} have been used for IMAC [18–22]. Among these metal cations, high-valence metal cation (e.g., Ti^{4+} and Zr^{4+}) immobilized IMAC materials stand out with the higher selectivity for phosphopeptides because of the unique coordination specificity of metal(IV)-phosphate chemistry [23]. Additionally, different metal ions may have different enrichment inclinations towards phosphopeptides, through different binding affinities. Thus, in Chen's group, complementary Fe^{3+}- and Ti^{4+}-immobilized metal ion affinity chromatography was employed to enrich phosphopeptides. And the phosphopeptides were analyzed more comprehensively with the above binary metal ions [24]. However, for the analysis of endogenous phosphopeptides from complex biosamples containing a large number of proteins, it is still a big challenge without appropriate mesoporous. Thus, it is important to fabricate a novel probe with not only multimetal cation affinity sites but also size-exclusion ability to isolate the endogenous phosphopeptides from complex biosamples.

The mesoporous silica materials were featured by controllable pore size, paintability in pore, and orderly pore size distribution. The paintability in channels gives them more functionalization for the wide range of usage [25–27]. The narrow channel distribution equipped the material with the selection to allow the infusion of small-size peptides and exclusion of large-size proteins outside simultaneously [28]. Thus, the mesoporous materials play an important role in the peptidomics analysis and were successfully applied in many reports for the enrichment of endogenous peptides. Zou and his co-workers fabricated a sandwich-like mesoporous material with ordered mesoporous silica structure, graphene, and carbon (denoted as graphene@$mSiO_2$-C) for the capture of common endogenous peptides, the resulting graphene@$mSiO_2$-C with large pore volume (0.587 $cm^3\ g^{-1}$), and the ordered narrow pore size (3 nm) showed excellent enrichment efficiency towards low-abundance common endogenous peptides in human serum. And after analyzed by LC-MS/MS, 892 common endogenous peptides were isolated from human serum by the graphene@$mSiO_2$-C nanocomposites [29]. In Su's group, adenosine phosphate-Ti^{4+}-functionalized MG@$mSiO_2$-ATP-Ti^{4+} mesoporous materials were employed to enrich endogenous phosphopeptides from complex biological samples. The ATP with three phosphate groups was coated on the inner wall of mesoporous channels for the immobilization of Ti^{4+} cations. With the excellent enrichment ability, 13 phosphopeptides and 19 endogenous phosphopeptides were successfully identified from nonfat milk and human saliva, respectively [6]. In our group, the hierarchically ordered macroporous/mesoporous silica nanohybrids (denoted as HOMMS@TiO_2) was designed facilely for the profiling of endogenous phosphopeptides in complex biosamples. The material with high surface area (255 m^2/g), sensitive detection (8 fmol), and rapid enrichment speed (within 1 min) were successfully employed to enrich endogenous phosphopeptides from complex biosample of human serum with high efficiency [13].

In this work, a novel mesoporous magnetic affinity probe with titania-zirconia binary metal cations (denoted as Fe_3O_4@$mSiO_2$@Ti^{4+}-Zr^{4+}) was synthesized for the endogenous phosphopeptides' enrichment. Facilely, the polydopamine was coated on the surface of Fe_3O_4@$mSiO_2$ nanoparticles. Afterwards, the metal cations Ti^{4+} and Zr^{4+} were grafted onto the dopamine integrally. The novel affinity probe possessed the advantages of size-exclusion effect which can enhance the selectivity towards small size of endogenous phosphopeptides, and dual metal cation affinity sites which can realize the identification of phosphopeptides comprehensively. With the above advantages, the nanocomposites were successfully used for the profiling of endogenous phosphopeptides in the human biofluids of saliva and aqueous fluid.

Experimental

Materials and reagents

Iron chloride hexahydrate ($FeCl_3 \cdot 6H_2O$), sodium acetate, ethylene glycol, NaOH, tetraethyl orthosilicate (TEOS), ethanol, and cetyltrimethylammonium bromide (CTAB) were bought from Shanghai Chemical Corp. Zirconium(IV) chloride, β-casein, α-casein, bovine serum albumin (BSA), and trypsin of bovine pancreas were bought from Sigma-Aldrich. Titanium (IV) sulfate was purchased from Adamas Reagent. ACN (HPLC-grade), 2,5-dihydroxybenzoic acid (DHB), and trifluoroacetic acid (TFA) were obtained from Merck (Darmstadt, Germany). All aqueous solutions were pretreated by Milli-Q system (Millipore, Bedford, MA). Additionally, all the other chemicals were of analytical grade.

Synthesis of Fe_3O_4@$mSiO_2$@Ti^{4+}-Zr^{4+}

The Fe_3O_4 nanoparticles were prepared according to the previous reports. Next, the obtained Fe_3O_4 nanoparticles were dispersed in 50 mL distilled water containing 500 mg

CTAB. After ultrasonication for about 30 min, 50 mL of 10 mM NaOH and 400 mL distilled water were furtherly mixed into the mixture which was stirred for 30 min at 60 °C. Next, 2.5 mL mixture of TEOS/ethanol (v/v 1:4) was instilled into the above solution. The resultant mixture was under the sustaining mechanical rabbling for about 12 h under 60 °C. After that, the products were separated and washed three times with distilled water and ethanol, respectively. Finally, the product was vacuum-dried at 50 °C and was then transferred to a muffle furnace with 350 °C for 4 h to dislodge CTAB. Finally, 10 mL of obtained Fe_3O_4@$mSiO_2$ nanoparticles was dispersed in the mixture of 20 mL ethanol and 10 mL Tris buffer (10 mM, deionized water as the solvent). Fifteen milliliters of dopamine hydrochloride aqueous solution (40 mg dopamine hydrochloride) was added into the above dispersion liquid. The mixture was mechanically stirred at room temperature for 20 min. After that, the obtained material Fe_3O_4@$mSiO_2$/PD was washed by deionized water and ethanol. Then, the obtained Fe_3O_4@$mSiO_2$/PD nanoparticles were dispersed in 100 mL 50 mM titanium (IV) sulfate and zirconium (IV) chloride aqueous. And the mixture was vibrated for 2 h. The Fe_3O_4@$mSiO_2$-Ti^{4+}-Zr^{4+} nanoparticles were rinsed thoroughly with deionized water and ethanol, followed by drying at 50 °C.

Synthesis of Fe_3O_4@$mSiO_2$@Ti^{4+} and Fe_3O_4@$mSiO_2$@Zr^{4+}

The workflow for the Fe_3O_4@$mSiO_2$@Ti^{4+} and Fe_3O_4@$mSiO_2$@Zr^{4+} nanocomposites' preparation was a resemblance with the preparation process of Fe_3O_4@$mSiO_2$@Ti^{4+}-Zr^{4+} nanocomposites, other than the amount of titanium sulfate was increased to 100 mL without zirconium chloride. And for Fe_3O_4@$mSiO_2$@Zr^{4+}, the amount of zirconium chloride was raised to 100 mL and without titanium sulfate addition. The procedures to fabricate mesoporous silica structure were similar to the preparation process of Fe_3O_4@$mSiO_2$@Ti^{4+}-Zr^{4+}.

Sample preparation

Firstly, 2 mg β-casein was dissolved into 500 μL of ammonium bicarbonate (50 mM, pH 8.3), and then, the protein solution was boiled in 100 °C water for about 8 min. Afterward, 2 mg/mL protein solution was obtained by adding 500 μL of Milli-Q water in the mixture. Finally, the trypsin (trypsin/protein, 1/40, w/w) was dissolved into the above protein solution and the solution was incubated sufficiently at 37 °C for 16–20 h.

The amount of 25 mg (0.16 mmol) DHB was dissolved into 1 mL buffer which comprised of 70%ACN/1% H_3PO_4.

Human saliva was collected from the morning salivary of a healthy volunteer. In brief, 2 mL saliva was mixed with 2 mL solution containing 0.2% TFA and the solution was centrifuged in 4 °C for 3 min under the speed of 8000 rpm. The supernatant was gathered for the biosample application.

Protocol of enrichment procedure

The workflow of phosphopeptide capture is demonstrated in Fig. 1. In brief, 200 μg Fe_3O_4@$mSiO_2$-Ti^{4+}-Zr^{4+} was mixed in 100 μL solution containing peptides which were diluted by 50%ACN/0.1%TFA, the resultant mixture was wobbled in a vortex at 37 °C for 30 min. Subsequently, the nanocomposites in the solution were separated from the supernatant surrounded by magnetic field. After discarding the supernatant, the nanocomposites was washed three times by the loading buffer (50%ACN/0.1%TFA). Next, the nanocomposites were dispersed in 10 μL 0.4 M ammonium hydroxide (v/v) and incubated at 37 °C for another 30 min. At last, the eluent containing enriched phosphopeptides was collected and analyzed with matrix-assisted laser desorption ionization time-of-flight mass spectrometry (MALDI-TOF-MS) or lyophilized for furtherly nano-LC-ESI-MS/MS analysis.

MS analysis and database search

All MALDI-TOF-MS experiments were carried out in a reflector positive mode by an AB Sciex 5800 MALDI-TOF mass spectrometer (AB Sciex, USA) with a Nd-YAG laser at 355 nm, frequency of 200 Hz, and acceleration voltage of 20 kV. A matrix solution of 2,5-dihydroxybenzoic acid (DHB, 10 mg/mL) was prepared in ACN/H_2O/TFA (50:50:0.1, v/v/v). Eluent (1 μL) was dropped on the MALDI plate and dried naturally. Then, 1 μL matrix solution was added and dried for mass analysis. More detailed information about nano-LC-MS/MS analysis and Database Search are shown in the Supporting Information.

Results and discussion

Synthesis and characteristics of Fe_3O_4@$mSiO_2$@Ti^{4+}-Zr^{4+} microspheres

The synthesis procedure of Fe_3O_4@$mSiO_2$@Ti^{4+}-Zr^{4+} nanocomposites is demonstrated in Fig. 2. Briefly, Fe_3O_4 nanoparticles were synthesized according to previous reports [30]. Then, mesoporous silica shell was prepared and coated on the Fe_3O_4 microsphere. Afterwards, dopamine was adhered to the surface of mesoporous silica shell. With the abundant hydroxyls, polydopamine can be used to immobilize metal cations Ti^{4+} and Zr^{4+}. Other than as the chelating ligand, polydopamine can also enhance the hydrophilicity of nanocomposites which can minimize some nonspecific adsorption.

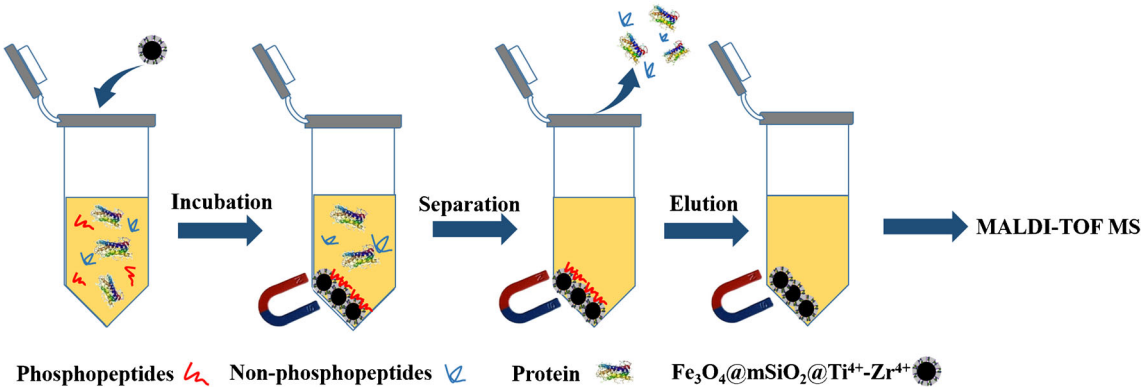

Fig. 1 Workflow of $Fe_3O_4@mSiO_2@Ti^{4+}$-Zr^{4+} probe for phosphopeptide enrichment from biological samples

Additionally, the whole fabricate procedure was carried out under moderate conditions (Fig. 2).

The characterization of $Fe_3O_4@mSiO_2@Ti^{4+}$-Zr^{4+} was carried out by various instruments. Firstly, transmission electron microscopy (TEM) images were employed to demonstrate the morphology of $Fe_3O_4@mSiO_2@Ti^{4+}$-Zr^{4+} microspheres. As can be seen in Fig. 3, the average diameter of Fe_3O_4 nanoparticles was around 300 nm; after the fabrication of mesoporous silica shell, a rough layer of mesoporous silica shell has been coated on the outermost of Fe_3O_4 cores successfully. After the modification of dopamine, the uniform pore channels can also be observed obviously.

Additionally, scanning electron microscope (SEM) with the energy dispersive spectrum and the chemical composition chart of $Fe_3O_4@mSiO_2@Ti^{4+}$-Zr^{4+} nanocomposites illustrated the existence of Zr and Ti, which indicated the successful immobilization of Ti^{4+} and Zr^{4+} ions onto the surface of $Fe_3O_4@mSiO_2$ (Fig. S1). Moreover, the TEM image and element analysis of $Fe_3O_4@mSiO_2@Ti^{4+}$ and $Fe_3O_4@mSiO_2@Zr^{4+}$ nanocomposites were also investigated. As can be seen in Fig. S2, the core-shell structure was well presented and the mesoporous channel can be observed clearly. The existence of O, C, Fe, Si, and Zr and the existence of O, C, Fe, Si, and Ti further verified the successful fabrication of $Fe_3O_4@mSiO_2@Ti^{4+}$ and $Fe_3O_4@mSiO_2@Zr^{4+}$ nanocomposites. The magnetic responsiveness of $Fe_3O_4@mSiO_2@Ti^{4+}$-Zr^{4+} nanoparticles was demonstrated by separating materials from distilled water when there is external magnetic field around. As shown in Fig. S3, $Fe_3O_4@mSiO_2@Ti^{4+}$-Zr^{4+} nanoparticles dispersed well in distilled water; after the magnet was applied beside the bottle, solid-liquid separation was realized within 30 s, and the result indicated the fast isolation ability of $Fe_3O_4@mSiO_2@Ti^{4+}$-Zr^{4+} from the solution.

Next, the nitrogen sorption was carried out to demonstrate the mesoporous structure of $Fe_3O_4@mSiO_2@Ti^{4+}$-Zr^{4+}. As can be seen in Fig. 4a, when the P/P_0 increased from 0.2 to 1.0, the adsorption volume increased in a curve, which was due to the occurrence of capillary condensation process under the high relative pressure. In general, the adsorption-desorption isotherms showed a typical IV-type curve of mesoporous structure. And the pore size distribution mainly focused on 4.0 nm (the inset in Fig. 4a); after the modification of polydopamine, the pore size was estimated to be about 3.7 nm (the inset in Fig. 4b), which demonstrated the mesoporous channels were retained after the immobilization of polydopamine. Besides, the BET surface area of $Fe_3O_4@mSiO_2@Ti^{4+}$-Zr^{4+} was about 197.27 m^2/g. All the above results implied the successful fabrication of $Fe_3O_4@mSiO_2@Ti^{4+}$-Zr^{4+} nanoparticles.

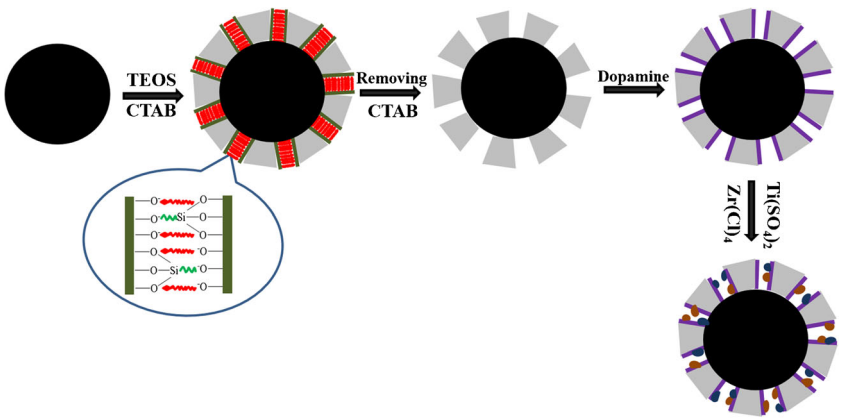

Fig. 2 Synthetic procedure of $Fe_3O_4@mSiO_2@Ti^{4+}$-Zr^{4+} microspheres

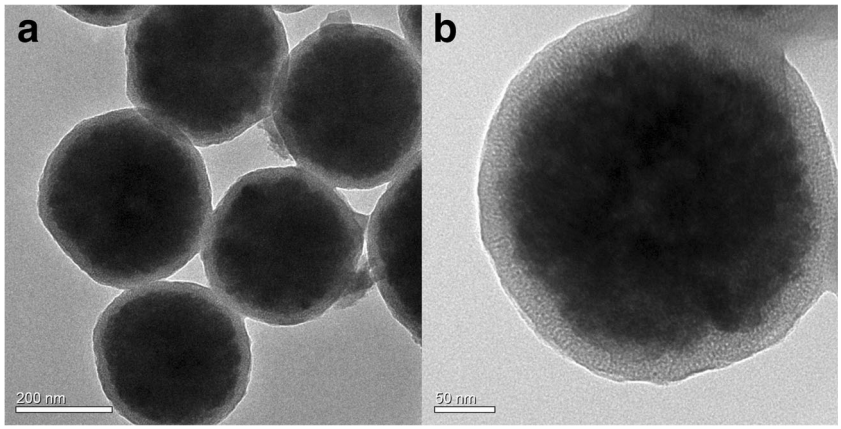

Fig. 3 Transmission electron microscopy (TEM) figures of Fe_3O_4@$mSiO_2$@Ti^{4+}-Zr^{4+} nanoparticles (**a**, **b**)

Evaluation of phosphopeptide enrichment performance by Fe_3O_4@$mSiO_2$@Ti^{4+}-Zr^{4+} probe

The enrichment procedure for phosphopeptides is illustrated in Fig. 1. Briefly, the procedure mainly contained four steps: incubation, separation, elution, and MS analysis. Utilizing the functional affinity probe, phosphopeptides were seized by metal cations and went through the mesoporous channels. In the washing step, large sizes of proteins and non-phosphopeptides were excluded out and washed away. At last, the eluent was analyzed by MALDI-TOF-MS without any treatment. To investigate the feasibility of using Fe_3O_4@$mSiO_2$@Ti^{4+}-Zr^{4+} for the endogenous phosphopeptides' enrichment, the phosphoprotein β-casein digest was employed as the standard sample. As shown in Fig. 5, the concentration of β-casein digests was 100 fmol/μL. Before the enrichment, barely no phosphopeptides were detected in mass spectrogram, for the existence of non-phosphopeptides can suppress the mass signal severely. However, after enriched by Fe_3O_4@$mSiO_2$@Ti^{4+}-Zr^{4+}, as can be seen in Fig. 5d, eight phosphopeptides including six mono-phosphopeptides and two multi-phosphopeptides were identified with high intensity. For comparison, affinity probe with mono-metal cations of Fe_3O_4@$mSiO_2$@Ti^{4+} and Fe_3O_4@$mSiO_2$@Zr^{4+} was fabricated to enrich phosphopeptides in the same way. As can be seen in Fig. 5 b and c, only five phosphopeptides including two multi-phosphopeptides and three mono-phosphopeptides were identified after enriching by Fe_3O_4@$mSiO_2$@Ti^{4+} and after captured by Fe_3O_4@$mSiO_2$@Zr^{4+}, five mono-phosphopeptides appeared on the mass spectrum without any multi-phosphopeptides. The results show the metal cation Ti^{4+} may have the enrichment inclination towards multi-phosphopeptides and the Zr^{4+} may have the enrichment inclination towards mono-phosphopeptides, which showed the same inclination with the metal oxides TiO_2 and ZrO_2 [31]. Thus, the binary metal cation–integrated mesoporous nanocomposites exhibited more comprehensive enrichment ability towards phosphopeptides and the detailed information could be found in Table S1.

Subsequently, we investigated the detection limit of Fe_3O_4@$mSiO_2$@Ti^{4+}-Zr^{4+} using the tryptic digests of β-casein with lower concentration. As shown in Fig. 6, before the enrichment, no phosphopeptides appeared in the mass spectrum. After being treated with Fe_3O_4@$mSiO_2$@Ti^{4+}-Zr^{4+}, four phosphopeptides were identified distinctly.

By contrast, when the affinity probe with single metal cations was applied to the enrichment, only two phosphopeptides

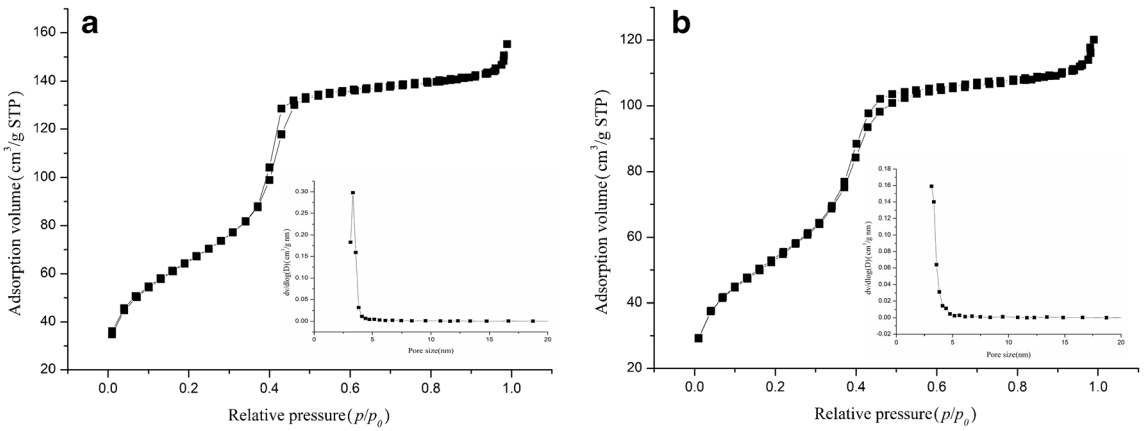

Fig. 4 Nitrogen adsorption-desorption isotherms of **a** Fe_3O_4@$mSiO_2$ and **b** Fe_3O_4@$mSiO_2$@Ti^{4+}-Zr^{4+}. The pore size distribution profile was inserted

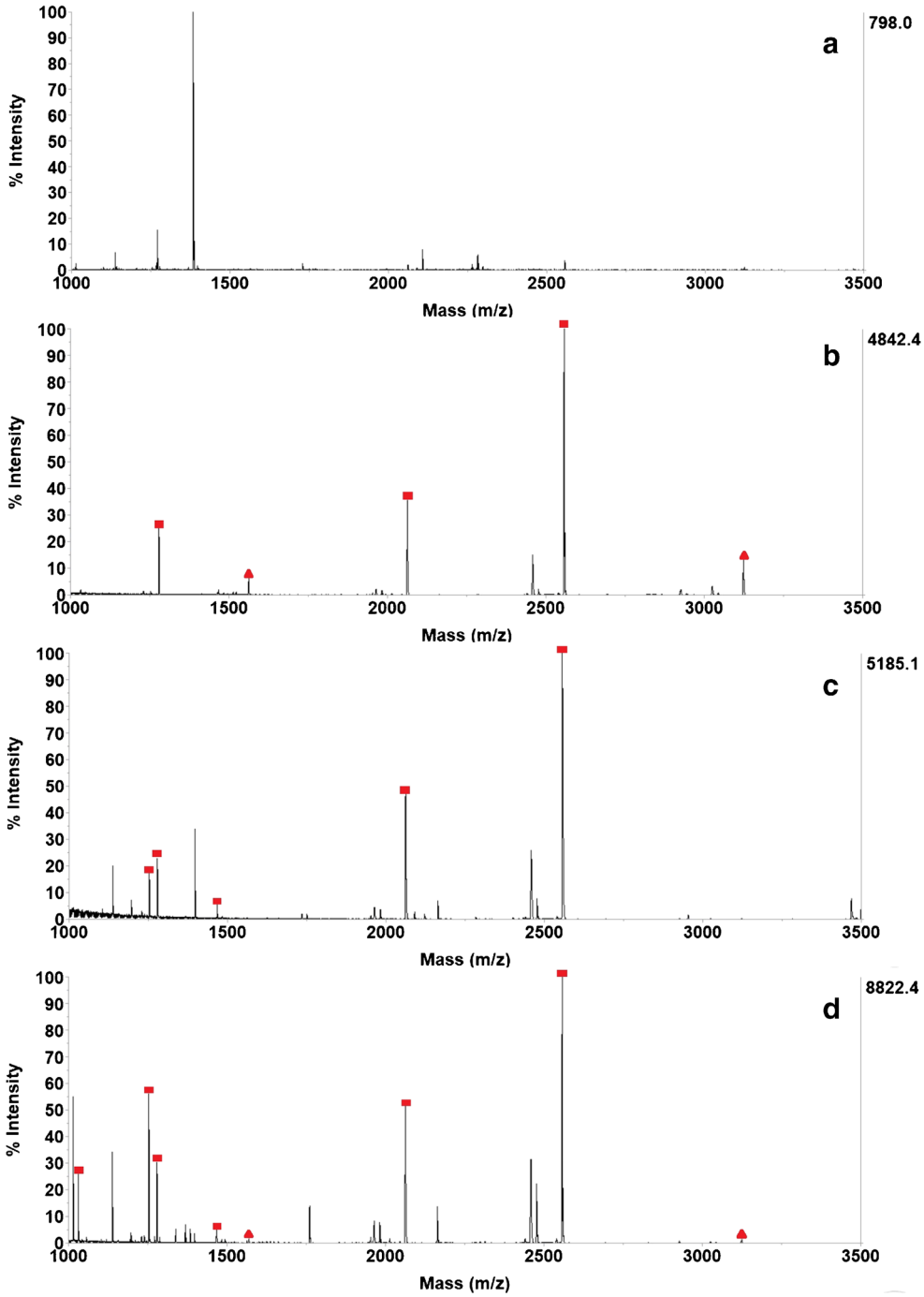

Fig. 5 Mass spectra of tryptic digested β-casein (100 fmol/μL) obtained **a** before enrichment and **b**–**d** after treatment with **b** Fe_3O_4@$mSiO_2$@Ti^{4+}, **c** Fe_3O_4@$mSiO_2$@Zr^{4+}, and **d** Fe_3O_4@$mSiO_2$@Ti^{4+}-Zr^{4+}. Mass spectrometric peaks of mono-phosphorylated peptides were labeled with red square, multi-phosphorylated peptides with triangles

were captured by Fe_3O_4@$mSiO_2$@Zr^{4+}. And only one phosphopeptide was enriched by Fe_3O_4@$mSiO_2$@Ti^{4+} with much low intensity and signal-to-noise ratio (S/N). Additionally, as can be seen in Fig. 7, even with the concentration of β-casein digest being as low as 0.1 fmol/μL, two phosphopeptides could still be observed after the enrichment by Fe_3O_4@$mSiO_2$@Ti^{4+}-Zr^{4+}. These results demonstrated the better enrichment ability of Fe_3O_4@$mSiO_2$@Ti^{4+}-Zr^{4+} than the probe of Fe_3O_4@$mSiO_2$@Zr^{4+} and Fe_3O_4@$mSiO_2$@Ti^{4+} with single metal cations towards phosphopeptides.

Furthermore, in view of the mesoporous structure, we employed the standard protein bovine serum albumin (BSA) and phosphorylated protein α-casein to investigate the size-exclusion effect of Fe_3O_4@$mSiO_2$@Ti^{4+}-Zr^{4+}. As shown in Fig. 8a, the mixture contained β-casein tryptic digests, BSA proteins, and α-casein protein and the mass ratio of β-casein tryptic digests/BSA protein/α-casein protein was 1:100:100.

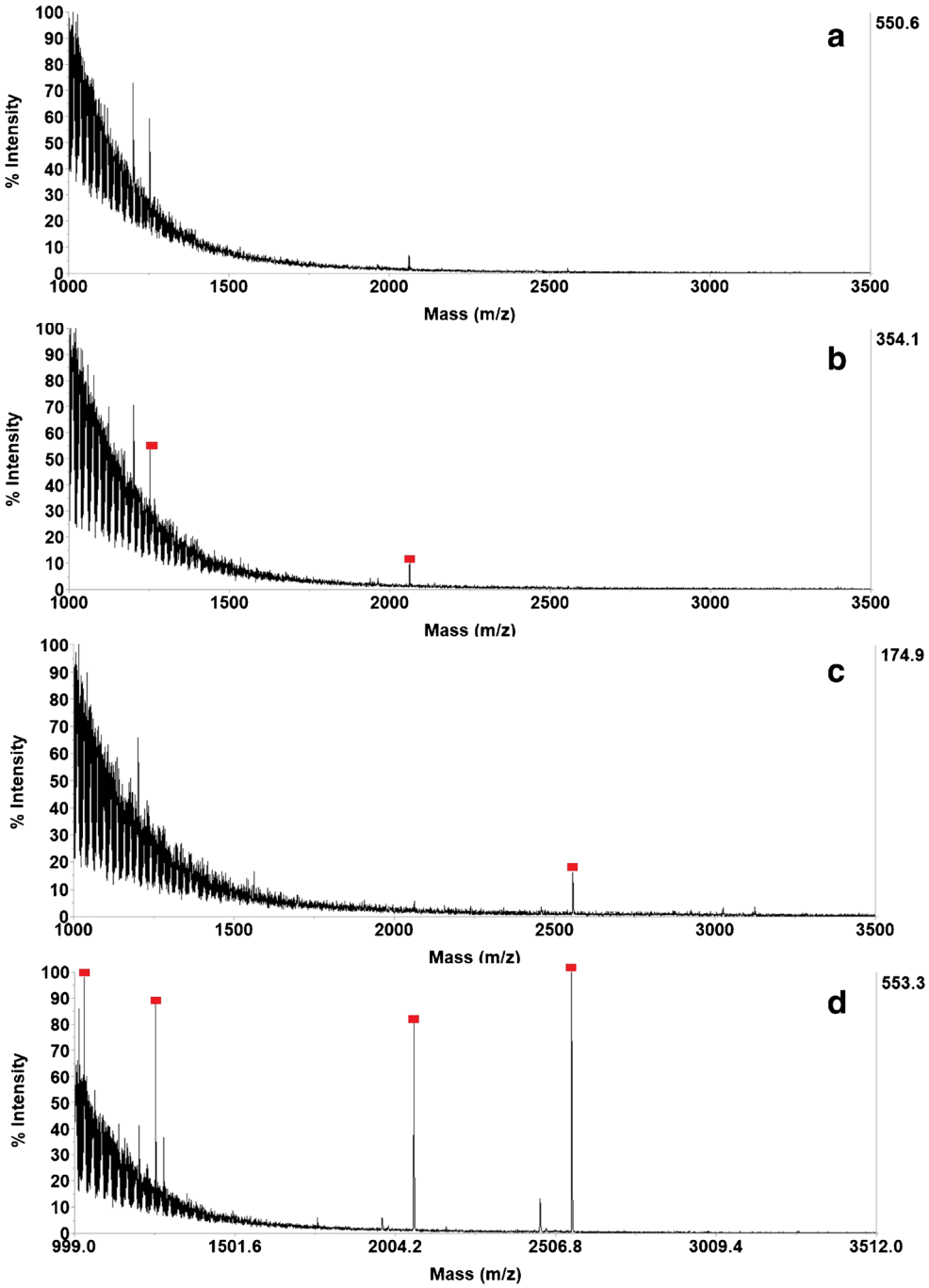

Fig. 6 Mass spectra of tryptic digested β-casein (2 fmol/μL) obtained **a** before enrichment and **b**–**d** after treatment with **b** Fe_3O_4@$mSiO_2$@Zr^{4+}, **c** Fe_3O_4@$mSiO_2$@Ti^{4+}, and **d** Fe_3O_4@$mSiO_2$@Ti^{4+}-Zr^{4+}. Mass spectrometric peaks of mono-phosphopeptides were labeled with red square, multi-phosphorylated peptides with triangles

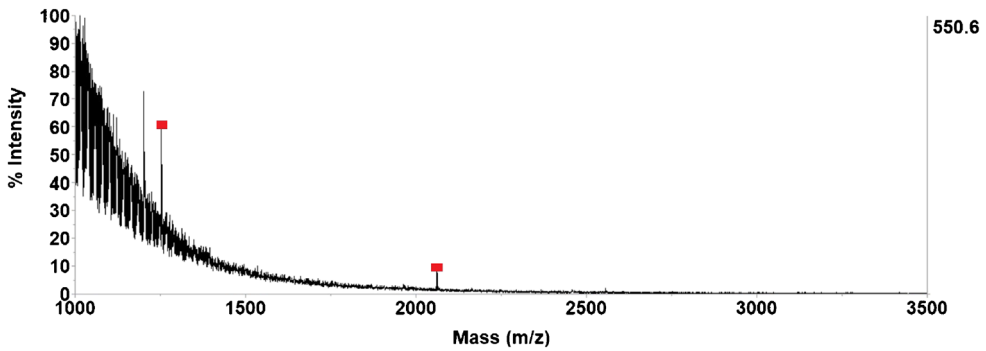

Fig. 7 MALDI-TOF mass spectra of tryptic digested β-casein (0.1 fmol/μL) after enriched by Fe_3O_4@$mSiO_2$@Ti^{4+}-Zr^{4+}. Mass spectrometric peaks of mono-phosphorylated peptides were marked with red square

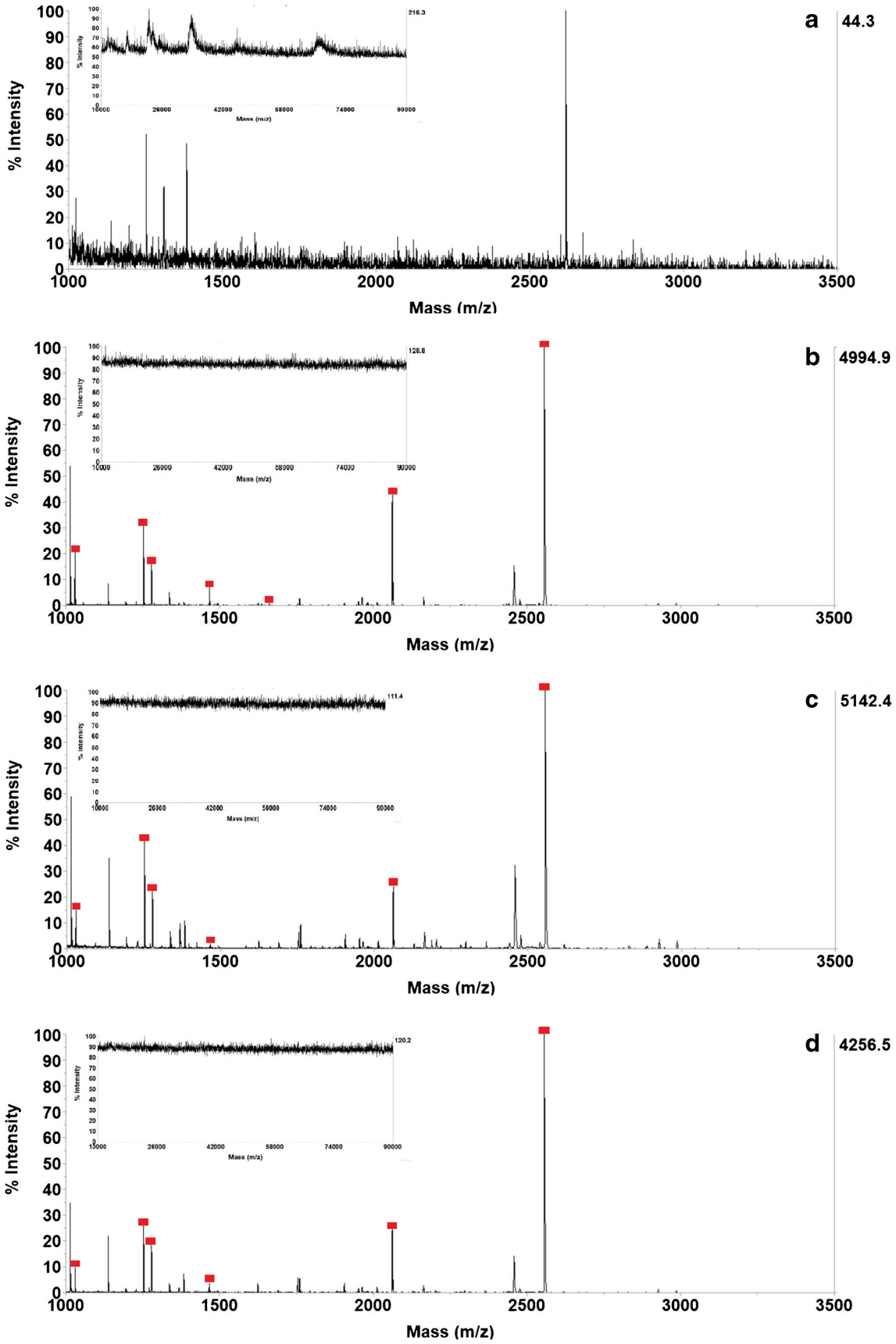
a
44.3
b
4994.9
c
5142.4
d
4256.5
% Intensity
Mass (m/z)

◀ **Fig. 8** Mass spectra of the mixture of β-casein tryptic digests, BSA protein, and α-casein protein with a mass ratio of **a** 1:100:100 before enrichment, **b** 1:100:100, **c** 1:500:500, and **d** 1:1000:1000 after enrichment by Fe_3O_4@$mSiO_2$@Ti^{4+}-Zr^{4+}. Mass spectrometric peaks of mono-phosphopeptides were labeled with red square

Before the enrichment, the peaks of proteins could be obviously observed (inset in Fig. 8a), and the peaks of phosphopeptides could hardly be identified due to the severe signal suppression by BSA proteins and α-casein proteins. While, after the enrichment with Fe_3O_4@$mSiO_2$@Ti^{4+}-Zr^{4+}, seven phosphopeptides were detected distinctly without any protein signals. When the interference increased to 1:500:500, a number of phosphopeptides could be identified and the protein signals vanished. Even with the increase of the mass ratio of β-casein tryptic digests/BSA protein/α-casein protein to 1:1000:1000, six phosphopeptides were still well distinguished on the spectrum without any protein peaks and the interference from non-phosphopeptides was extremely low. These results demonstrated the large concentration of phosphorylated proteins and non-phosphorylated proteins would not influence the enrichment of Fe_3O_4@$mSiO_2$@Ti^{4+}-Zr^{4+} nanocomposites which could be ascribed to the uniform mesoporous structures on the outermost position of the nanocomposites. Thus, the results indicated the excellent size-exclusion ability of the materials and the great potential for the application of Fe_3O_4@$mSiO_2$@Ti^{4+}-Zr^{4+} in the endogenous phosphopeptides profiling furtherly.

Also, the reusability of the materials was investigated by treating β-casein tryptic digests. The nanocomposites were reused for five times. Before each enrichment cycle, the nanocomposites were washed with eluent and loading buffer several times to remove the residual phosphopeptides and non-phosphopeptides thoroughly. As shown in Fig. S4, after repeating the enrichment cycles for five times, the analytical performance had no significant difference during the sequential five enrichment cycles. Eight phosphopeptides (m/z 1030.9, 1253.1, 1278.6, 1466.5, 1562.0, 3123.0, 2556.8, 2061.6) were identified along the five enrichment cycles with the similar intensity. The results demonstrated the good reproducibility and stability of Fe_3O_4@$mSiO_2$@Ti^{4+}-Zr^{4+} nanocomposites.

Encouraged by all the above results, we employed the Fe_3O_4@$mSiO_2$@Ti^{4+}-Zr^{4+} nanocomposites to enrich endogenous phosphopeptides from complex human biofluids without enzymolysis. Human saliva, as one of the most important human fluids, has the merits of easy collection and noninvasiveness. Thus, it has been extensively used as biosamples for the clinical diagnosis. As can be seen in Fig. 9a, before the enrichment, few endogenous phosphopeptides could be identified, and the mass spectrum peaks were severely suppressed by non-phosphopeptides and large size of proteins. However, after treatment with Fe_3O_4@$mSiO_2$@Ti^{4+}-Zr^{4+}, 13 endogenous phosphopeptides including 11 mono- and 2 multi-phosphopeptides were detected distinctly with high intensity. These peaks had been testified to be phosphopeptides by MALDI-MS/MS (Fig. S5). Moreover, human aqueous fluid as a complex biosample was also analyzed for the endogenous phosphopeptides in this work. After being analyzed by nano-LC-ESI-MS/MS, totally 104 endogenous phosphopeptides containing 9 multi-

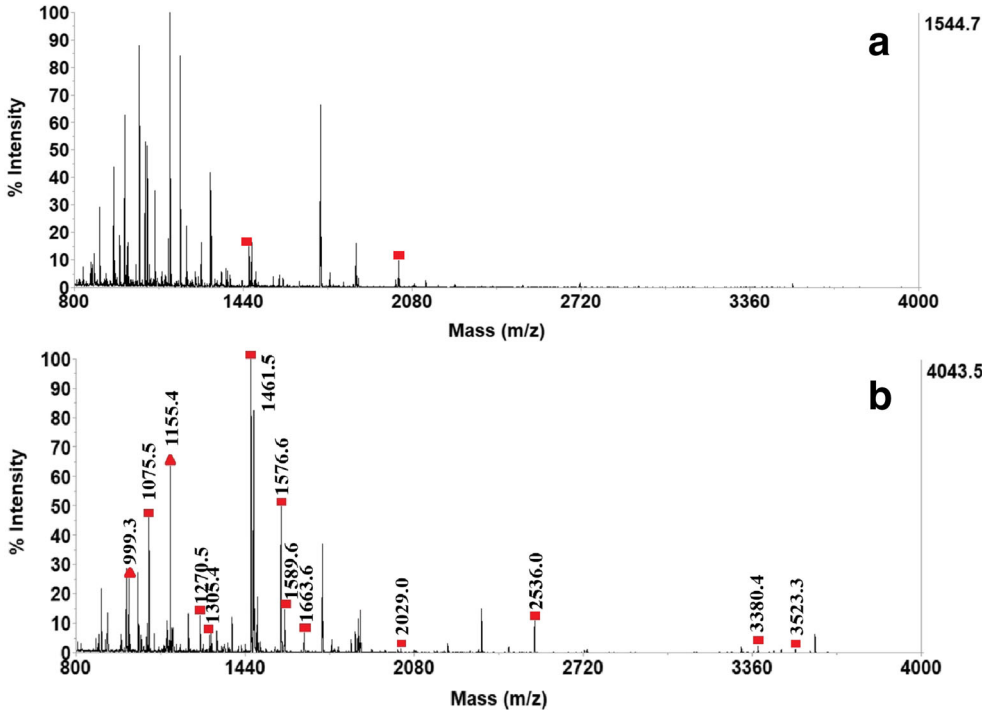

Fig. 9 Mass spectra of endogenous phosphopeptides enriched from human saliva **a** without enrichment and **b** after enriched by Fe_3O_4@$mSiO_2$@Ti^{4+}-Zr^{4+}. Mass spectrometric peaks of mono-phosphopeptides were labeled with red square, multi-phosphorylated peptides with triangles

and 95 mono-phosphopeptides were identified from 10 μL pristine human saliva and 4 endogenous phosphopeptides were identified from 10 μL human aqueous fluid, respectively. And the detailed information could be found in Table S2 and S3, respectively. Compared with previous reports [4, 32, 33], the Fe_3O_4@mSiO_2@Ti^{4+}-Zr^{4+} nanocomposites exhibited great efficiency in detecting endogenous phosphopeptides from complex human biofluids. Moreover, we furtherly analyzed the precursor proteins of the endogenous phosphopeptides captured from human saliva; most endogenous phosphopeptides are from salivary acidic proline-rich phosphoproteins. The acidic proline-rich proteins can bind calcium potently and inhibit the crystal growth of calcium phosphates. Thus, they can prevent the formation of hydroxyapatite on the tooth surface and provide a protective and reparative environment for dental enamel which is important for the integrity of the teeth [34]. Also, a number of endogenous phosphopeptides' precursor protein are basic salivary proline-rich protein. And in Lamkin's work, the specific basic proline-rich proteins in human parotid saliva were proved to possess significant anti-HIV-1 activity [35]. Thus, the identification of endogenous phosphopeptides in human biofluids has great significance for the disease researches and diagnosis.

Conclusion

In this work, a novel affinity probe Fe_3O_4@mSiO_2@Ti^{4+}-Zr^{4+} nanocomposite was successfully synthesized and employed to enrich endogenous phosphopeptides from human biofluids. The as-synthesized Fe_3O_4@mSiO_2@Ti^{4+}-Zr^{4+} has the advantages of bimetallic affinity site from Ti^{4+} and Zr^{4+}, uniform mesoporous structure, and good superparamagnetism. Additionally, the modified form of bimetallic ions on the mesoporous channels increased the exposure of affinity sites and realized a more convenient and replaceable multifunctional modified form. In comparison with the single metal centered materials (Fe_3O_4@mSiO_2@Zr^{4+} and Fe_3O_4@mSiO_2@Ti^{4+}), Fe_3O_4@mSiO_2@Ti^{4+}-Zr^{4+} could detect phosphopeptides including mono- and multi-phosphorylated peptides more comprehensively and exhibited better sensitivity and selectivity. Finally, the novel affinity was successfully employed to enrich endogenous phosphopeptides from human saliva and human aqueous fluid, suggesting its further potential in pretreatment of human biofluids for the peptidome researches and disease diagnosis.

Funding information This work was financially supported by the National Natural Science Foundation of China (21425518, 21405022, and 21675034) and National Basic Research Priorities Program of China (2013CB911201).

Compliance with ethical standards

Conflict of interest The author(s) declare that they have no competing interests.

References

1. La Barbera G, Capriotti AL, Cavaliere C, Ferraris F, Laus M, Piovesana S, Sparnacci K, Laganà A (2018) Development of an enrichment method for endogenous phosphopeptide characterization in human serum. Anal Bioanal Chem 410:1177–1185
2. Marshall J, Kupchak P, Zhu W, Yantha J, Vrees T, Furesz S, Jacks K, Smith C, Kireeva I, Zhang R, Takahashi M, Stanton E, Jackowski G (2003) Processing of serum proteins underlies the mass spectral fingerprinting of myocardial infarction. J Proteome Res 2:361–372
3. Dallas DC, Guerrero A, Parker EA, Robinson RC, Gan J, German JB, Barile D, Lebrilla CB (2015) Current peptidomics: applications, purification, identification, quantification, and functional analysis. Proteomics 15:1026–1038
4. Liu Q, Sun N, Gao M, Deng C-h (2018) Magnetic binary metal–organic framework as a novel affinity probe for highly selective capture of endogenous phosphopeptides. ACS Sustain Chem Eng 6:4382–4389
5. Beltran L, Cutillas PR (2012) Advances in phosphopeptide enrichment techniques for phosphoproteomics. Amino Acids 43:1009–1024
6. Su J, He X, Chen L, Zhang Y (2018) Adenosine phosphate functionalized magnetic mesoporous graphene oxide nanocomposite for highly selective enrichment of phosphopeptides. ACS Sustain Chem Eng 6:2188–2196
7. Boersema PJ, Mohammed S, Heck AJR (2009) Phosphopeptide fragmentation and analysis by mass spectrometry. J Mass Spectrom 44:861–878
8. Lin H, Chen H, Shao X, Deng C (2018) A capillary column packed with a zirconium(IV)-based organic framework for enrichment of endogenous phosphopeptides. Microchim Acta 185:562
9. Li Y, Liu L, Wu H, Deng C (2019) Magnetic mesoporous silica nanocomposites with binary metal oxides core-shell structure for the selective enrichment of endogenous phosphopeptides from human saliva. Anal Chim Acta 1079:111–119
10. Villanueva J, Philip J, Entenberg D, Chaparro CA, Tanwar MK, Holland EC, Tempst P (2004) Serum peptide profiling by magnetic particle-assisted, automated sample processing and MALDI-TOF mass spectrometry. Anal Chem 76:1560–1570
11. Lan X, Liao D, Wu S, Wang F, Sun J, Tong Z (2015) Rapid purification and characterization of angiotensin converting enzyme inhibitory peptides from lizard fish protein hydrolysates with magnetic affinity separation. Food Chem 182:136–142
12. Yao J, Sun N, Deng C, Zhang X (2015) Designed synthesis of graphene @titania @mesoporous silica hybrid material as size-exclusive metal oxide affinity chromatography platform for selective enrichment of endogenous phosphopeptides. Talanta 150:296–301
13. Yan Y, Zhang X, Deng C (2014) Designed synthesis of titania nanoparticles coated hierarchically ordered macro/mesoporous silica for selective enrichment of phosphopeptides. ACS Appl Mater Interfaces 6:5467–5471
14. Chen CT, Chen YC (2005) Fe3O4/TiO2 Core/shell nanoparticles as affinity probes for the analysis of phosphopeptides using TiO2 surface-assisted laser desorption/ionization mass spectrometry. Anal Chem 77:5912–5919

15. Yan Y, Zheng Z, Deng C, Zhang X, Yang P (2013) Facile synthesis of Ti4+−immobilized Fe3O4@polydopamine core-shell microspheres for highly selective enrichment of phosphopeptides. Chem Commun 49:5055–5057
16. Qi D, Mao Y, Lu J, Deng C, Zhang X (2010) Phosphate-functionalized magnetic microspheres for immobilization of Zr4+ ions for selective enrichment of the phosphopeptides. J Chromatogr A 1217:2606–2617
17. Andersson L, Porath J (1986) Isolation of phosphoproteins by immobilized metal (Fe3+) affinity chromatography. Anal Biochem 154:250–254
18. Kinoshita E, Kinoshita-Kikuta E, Takiyama K, Koike T (2006) Phosphate-binding tag, a new tool to visualize phosphorylated proteins. Mol Cell Proteomics 5:749–757
19. Hu Q, Hu S, Zhang Z, Zhou X, Yang S, Zhang Y, Chen X (2011) Fe3+−immobilized nanoparticle-modified capillary for capillary electrophoretic separation of phosphoproteins and non-phosphoproteins. Electrophoresis 32:2867–2873
20. Posewitz MC, Tempst P (1999) Immobilized gallium(III) affinity chromatography of phosphopeptides. Anal Chem 71:2883–2892
21. Ficarro SB, Adelmant G, Tomar MN, Zhang Y, Cheng VJ, Marto JA (2009) Magnetic bead processor for rapid evaluation and optimization of parameters for phosphopeptide enrichment. Anal Chem 81:4566–4575
22. Yu Z, Han G, Sun S, Jiang X, Chen R, Wang F, Wu R, Ye M, Zou H (2009) Preparation of monodisperse immobilized Ti4+ affinity chromatography microspheres for specific enrichment of phosphopeptides. Anal Chim Acta 636:34–41
23. Han G, Ye M, Zou H (2008) Development of phosphopeptide enrichment techniques for phosphoproteome analysis. Analyst. 133: 1128–1138
24. Lai ACY, Tsai CF, Hsu CC, Sun YN, Chen YJ (2012) Complementary Fe3+- and Ti4+-immobilized metal ion affinity chromatography for purification of acidic and basic phosphopeptides. Rapid Commun Mass Sp 26:2186–2194
25. Sun N, Deng C, Li Y, Zhang X (2014) Size-exclusive magnetic graphene/mesoporous silica composites with titanium(IV)-immobilized pore walls for selective enrichment of endogenous phosphorylated peptides. ACS Appl Mater Interfaces 6:11799–11804
26. Yin P, Wang Y, Li Y, Deng C, Zhang X, Yang P (2012) Preparation of sandwich-structured graphene/mesoporous silica composites with C8-modified pore wall for highly efficient selective enrichment of endogenous peptides for mass spectrometry analysis. Proteomics 12:2784–2791
27. Zhu GT, Li X-S, Gao Q, Zhao N-W, Yuan B-F, Feng Y-Q (2012) Pseudomorphic synthesis of monodisperse magnetic mesoporous silica microspheres for selective enrichment of endogenous peptides. J Chromatogr A 1224:11–18
28. Tian R, Zhang H, Ye M, Jiang X, Hu L, Li X, Bao X, Zou H (2010) Selective extraction of peptides from human plasma by highly ordered mesoporous silica particles for peptidome analysis. Angew Chem Int Ed 46:962–965
29. Zhang Q, Xiong Z, Wan H, Chen X, Zou H (2016) Facile preparation of mesoporous carbon-silica-coated graphene for the selective enrichment of endogenous peptides. Talanta 146:272–278
30. Long X-y, Li J-y, Sheng D, Lian H-Z (2016) Low-cost iron oxide magnetic nanoclusters affinity probe for the enrichment of endogenous phosphopeptides in human saliva. RSC Adv 6:96210–96222
31. Kweon HK, Håkansson K (2006) Selective zirconium dioxide-based enrichment of phosphorylated peptides for mass spectrometric analysis. Anal Chem 78:1743–1749
32. Yao J, Sun N, Wang J, Xie Y, Deng C, Zhang X (2017) Rapid synthesis of titanium(IV)-immobilized magnetic mesoporous silica nanoparticles for endogenous phosphopeptides enrichment. Proteomics 17:1600320
33. Wu Y, Liu Q, Xie Y, Deng C (2018) Core-shell structured magnetic metal-organic framework composites for highly selective enrichment of endogenous N-linked glycopeptides and phosphopeptides. Talanta 190:298–312
34. Bennick A (1982) Salivary proline-rich proteins. Mol Cell Biochem 45:83–99
35. Robinovitch MR, Ashley RL, Iversen JM, Vigoren EM, Lamkin M (2001) Parotid salivary basic proline-rich proteins inhibit HIV-I infectivity. Oral Dis 7:86–93